Supplement of Atmos. Meas. Tech., 14, 5555–5576, 2021
https://doi.org/10.5194/amt-14-5555-2021-supplement

Atmospheric Measurement Techniques
Open Access
EGU

Supplement of

Boundary layer water vapour statistics from high-spatial-resolution spaceborne imaging spectroscopy

Mark T. Richardson et al.

Correspondence to: Mark T. Richardson (markr@jpl.nasa.gov)

1 Clear- versus all-sky statistics

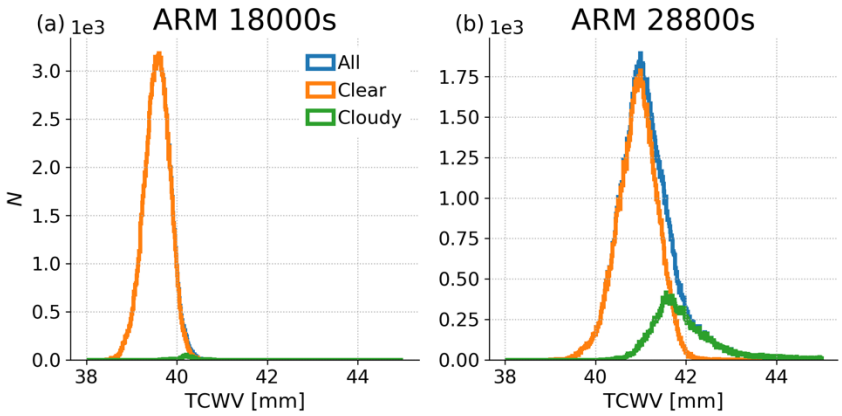

Figure S1. Histograms of TCWV for all columns in (a) the 18000 second snapshot of the ARM LES and (b) the 28800 s snapshot of the same. The blue histograms show all columns, the orange histograms the clear-sky only (defined as estimated $\tau_{cloud} < 0.3$) and the green the cloudy-sky footprints. Cloud fraction increases from 0.7 % to 21.1 % between the snapshots.

2 Use of simplified forward model in retrieval

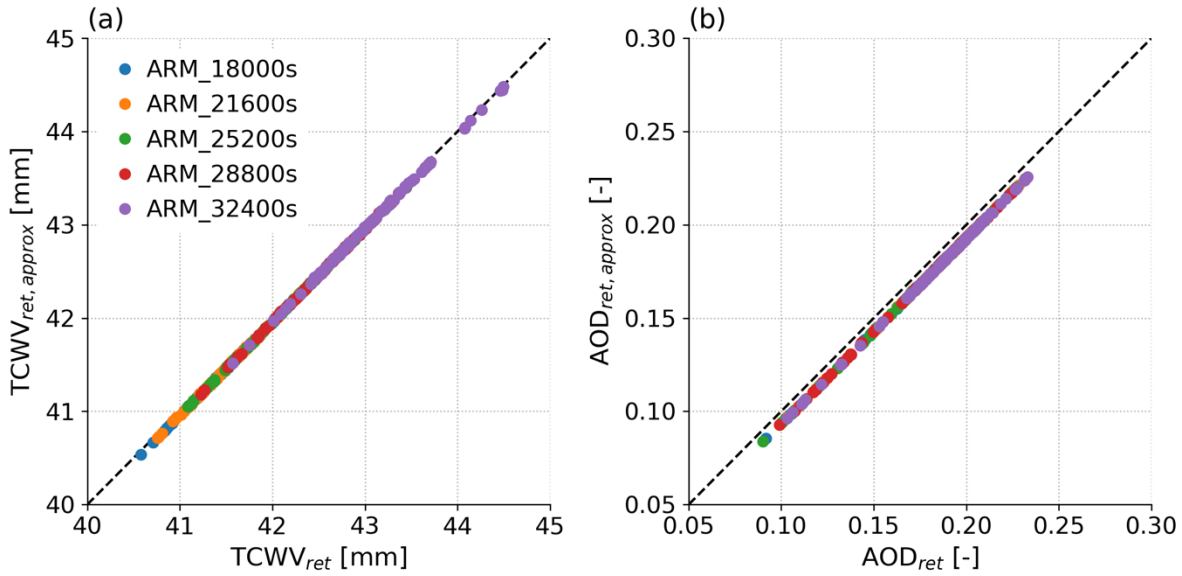

Figure S2. (a) retrieved TCWV and (b) retrieved AOD when using the forward model approximation as a function of the same retrieved values when providing MODTRAN with the surface ρ_s spectrum as input. For the same *N*=101 footprints as in the main paper and a subset of ARM snapshots.

3 Prior TCWV tests

Figure S3 shows how retrieved TCWV and surface change when the TCWV prior is changed from 40 mm to 7.5 mm. This is prior change goes outside any of the TCWV in our LES so is quite an extreme test, smaller changes in prior (e.g. to 30 mm, not shown) cause smaller shifts in retrieved properties. Mean retrieved TCWV changes by approximately 0.15 mm and there is no significant change in any trend or standard deviation. For example, the worst case is over the darkest surface where signal-to-noise ratio is lower. In this case the trend between the retrievals with each prior is 1.00±0.04 and the change in standard deviation is 0.00±0.04 mm. While there is a small difference in mean retrieved properties, there is no detectable change in standard deviation or the gradient between the two, so we expect no changes in the emulator a_1 parameter and therefore no effect on our conclusions or reported results from this prior choice. Results are similar using other snapshots and MODTRAN Cropland surface (not shown).

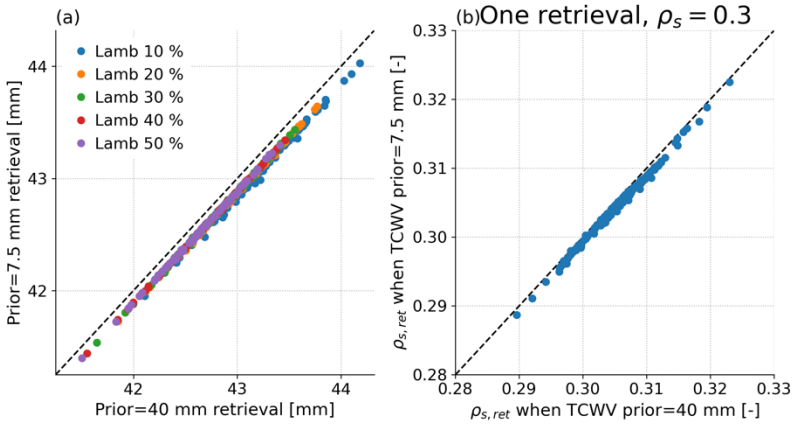

Figure S3. (a) Retrieved TCWV using a prior of 7.5 mm versus when using 40 mm for ARM_18000s atmosphere with Lambertian surfaces with ρ_s from 0.1—0.5. (b) Example of retrieved surface reflectance for each channel for one retrieval with each prior in a ρ_s=0.3 case.

4 Sample size and emulator fits

The main manuscript emulators used 303—707 data points, with 101 from each snapshot in the relevant case. It was not known *a priori* that the snapshots could be combined, so we required a sample size that would produce stable emulator parameters from a single snapshot. This was confirmed by incrementally increasing sample size and fitting emulator parameters until the parameters stabilised such that a larger sample size did not change the results. This is confirmed for ARM_18000s in Figure S4, where parameters stabilise below N=101. These results are characteristic of other snapshots (not shown).

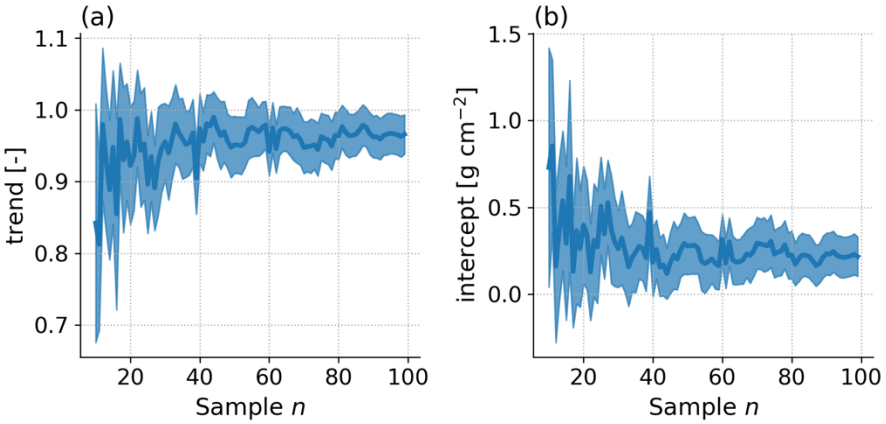

Figure S4. (a) slope and (b) intercept parameters from linear fits between TCWV and $TCWV_{ret}$ in ARM_18000s for random subsamples of footprints with increasing sample size.

5 Solar zenith angle tests

The 101 footprints from ARM_18000s were simulated and retrieved as in the main manuscript but for SZAs of 14°, 30°, 45° and 60°, each with its own lookup table. The forward model was the simplified Lambertian Eq. (1) with a MODTRAN cropland surface underneath, and the lookup table used the midlatitude summer atmosphere. Figure S5 shows how each of the other SZA retrievals relates to those at SZA=45°. More scatter is visible at SZA=60°, and the statistics of the emulator parameters a_1 (gradient $dTCWV_{ret}/dTCWV_{true}$) and σ_ε (standard deviation of residuals) are listed in Table S1. The a_1 values are all statistically indistinguishable, and their best fits differ by ~3 %, which is small relative to the differences between LES cases. Random error increases in magnitude with SZA, but this difference is only significant at 2σ between SZA=60° and SZA≤45°. The Table S1 values of a_1 differ from the ARM trends in main manuscript Table 2, but this is not significant and happens because Table 2 uses all ARM snapshot footprints, rather than just ARM_18000s.

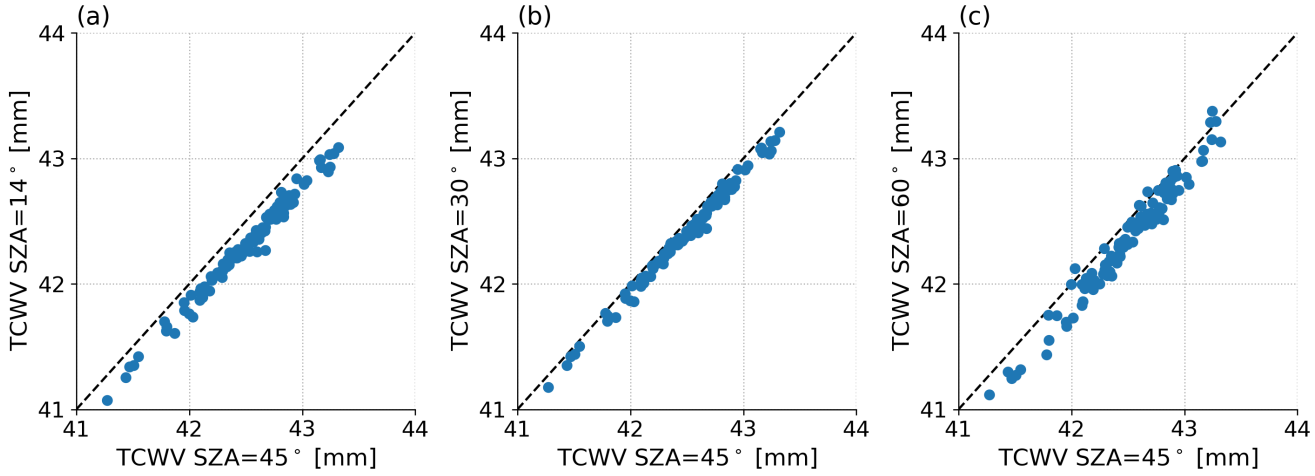

Figure S5. Retrieved TCWV for the ARM_18000s snapshot as SZA varies, plotted as a function of the retrieved value at SZA=45°. (a) SZA=14°, (b) SZA=30°, (c) SZA=60°

Table S1.

	Best estimate±2σ	
SZA	a_1 [mm mm^{-1}]	σ_ε [mm]
60	1.058±0.148	0.263±0.037
45	1.029±0.118	0.209±0.030
30	1.023±0.107	0.189±0.027
14	1.021±0.102	0.181±0.026

6 Aerosol optical depth and water vapour retrieval co-dependence

A coding error assigned AOD=0.2 to most footprints rather than evenly sampling from AOD of 0.1—0.2. Figure S6 shows that the AOD retrieval performs well over vegetated surfaces, but that darker and flatter surface ρ_s spectra degrade the correlation, bias and spread. Comparing panels (e,f) with their associated surfaces (b,c), the retrieval generally compensates for darker surfaces by increasing the AOD. This larger simulated AOD likely explains the λ<800 nm curvature in the retrieved ρ_s for the 10 % and 20 % Lambertian surfaces. Additionally, darker and flatter surface spectra are associated with a loss of correlation between AOD and AOD_{ret}. This confirms unsurprising relationships between retrieved AOD and ρ_s, but the question of interest for this study is whether the relationship between TCWV and $TCWV_{ret}$ is strongly affected by AOD.

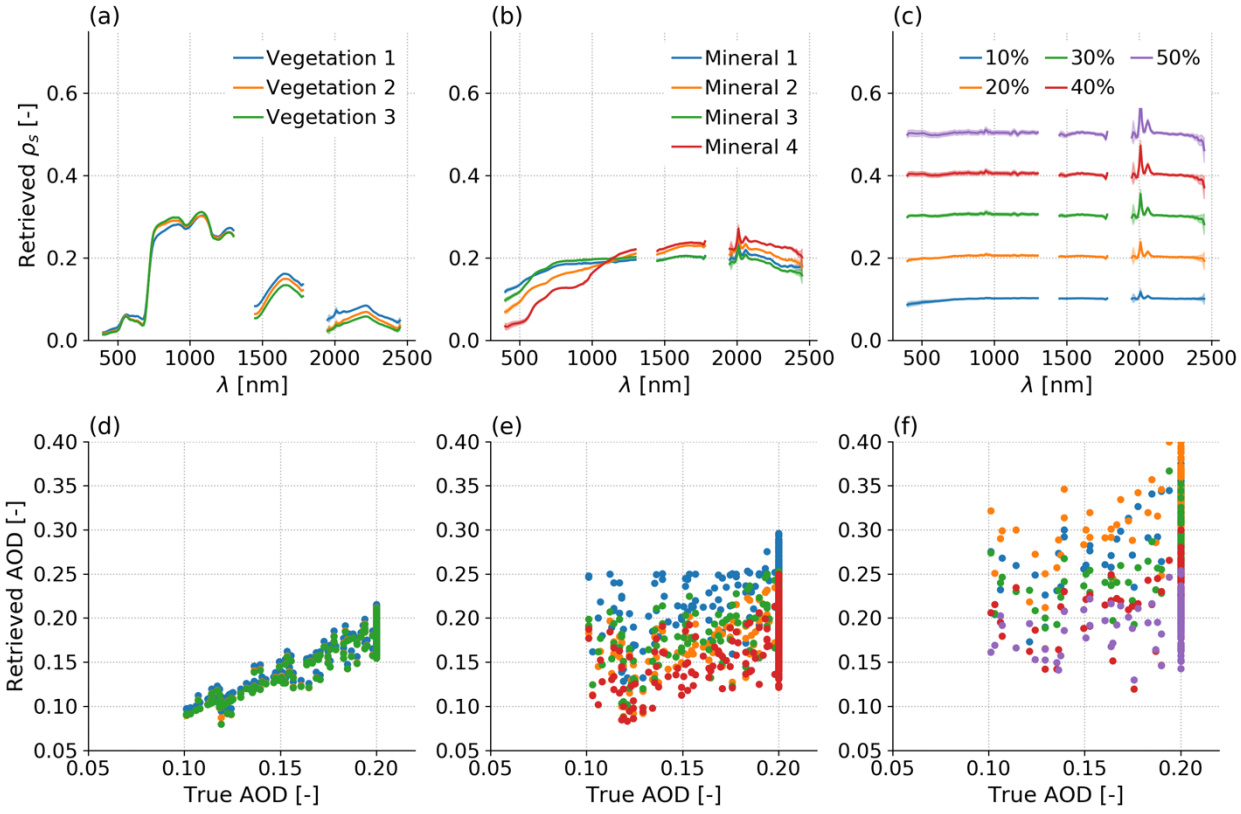

Figure S6. As main text Figure 4 but (d—f) have been replaced with retrieved AOD as a function of true AOD.

Figure S7 shows that the $TCWV_{ret}$ bias differences between snapshots are far larger than any shift induced by background AOD, and also shows the emulator trend parameters calculated for each LES case when separately fitting to footprints with AOD=0.2 or AOD<0.2. There is a significant difference (p<0.05) in ARM_lsconv but no others. This is evidence that in some cases, changes in background AOD could affect derived spatial statistics, but once again, the differences induced by AOD are substantially smaller than those caused by different meteorological conditions or surface type. We also considered $TCWV_{ret}$ minus TCWV as a function of AOD_{ret} minus AOD, but results were very similar to panel (a).

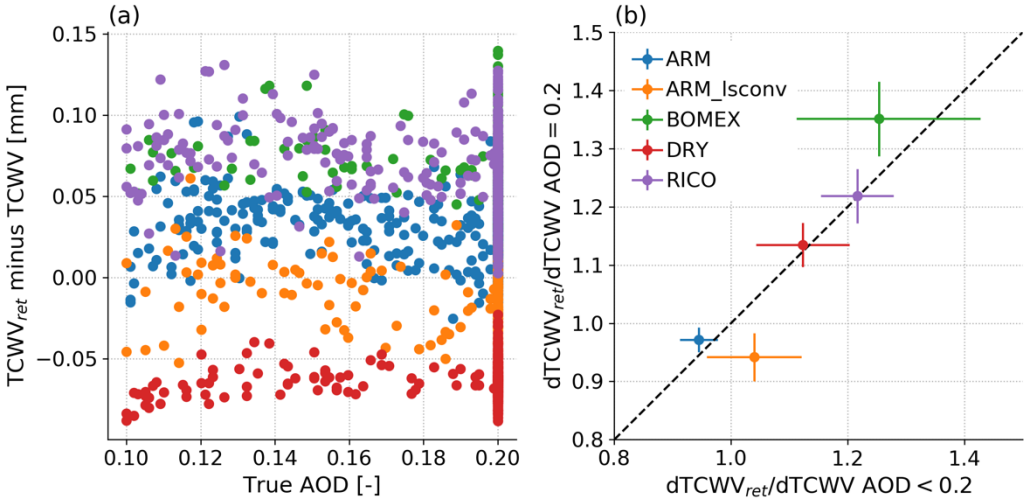

Figure S7. (a) Footprint $TCWV_{ret}$ minus true TCWV as a function of true AOD (b) Slopes±2σ error of $TCWV_{ret}$ regressed against TCWV for the subset in each case with AOD=0.2 versus the subset with AOD<0.2. Differences are significant at 2σ when the ellipse defined by the error bars is not intersected by the dashed 1:1 line. This is only true for ARM_lsconv.

7 Emulators fit to individual snapshots versus all snapshots in a case

Emulators were fit to each of the individual snapshots and their best fit parameters compared with those obtained from fits to the full snapshot datasets. While individual snapshots will clearly differ somewhat, we question whether these differences are likely to be substantial and whether they can be detected with significance.

Of the 23 snapshots, Figure S8 shows that 2 had significant ($p<0.05$) differences in a_1 (slope) and a_2 (intercept), and zero had differences in σ_ε (random error). From a sample of 23, the 95 % confidence interval of the number of samples that will be different at 2σ is 0—4, so we do not have evidence of systematic differences between the emulators fit to individual snapshots versus individual cases. This contrasts with the differences between cases, where there are more significant differences. We note that some of the best-fit differences are substantial, particularly DRY_7200s and DRY_10800s, but this is because they show small spread in TCWV and therefore large uncertainty in their estimated $dTCWV_{ret}/dTCWV$.

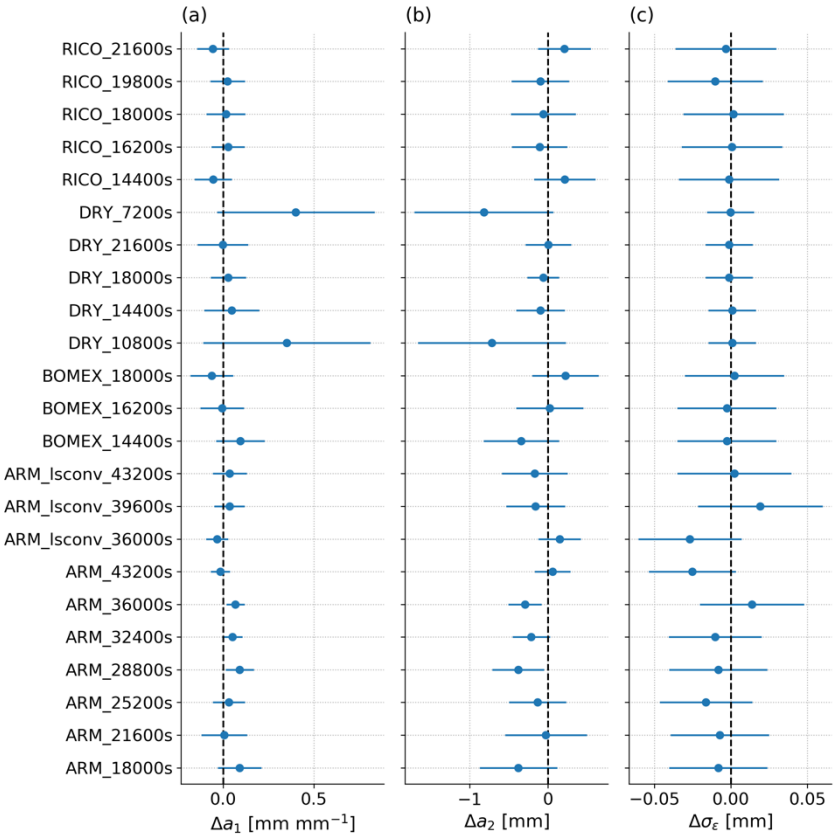

Figure S8. Differences in emulator parameters for each snapshot relative to those calculated using all snapshots in each case. (a) slope parameter a_1, (b) intercept parameter a_2, (c) standard deviation of residuals σ_ε. In all cases the points are best estimates, the error bars are 2σ and differences of zero are shown by vertical dashed lines.

8 Estimating random retrieval error

The retrieved TCWV field variance consists of the sum of the true field variance (σ_x^2) and the retrieval error variance (σ_ϵ^2). We desire an accurate estimate of σ_ϵ^2 so that we can remove it and obtain σ_x^2. Our method exploits how the water vapour field is relatively uniform over short distance ranges. The main manuscript phrases this mathematically, here we show the approach schematically and compare its performance with an alternative smoothing-based estimate. Our approach treats the x and y directions differently by separately considering each "strip" of LES grid cells in the y direction as shown in Figure S9. The water vapour values vary roughly from 39—40.5 mm in both the LES raw output and in the retrieved field. However, the inset shows that on smaller spatial scales the LES TCWV field is more spatially smooth than the retrieved TCWV field, since σ_x^2 is small over very short horizontal distances, but σ_ϵ^2 is constant at all scales.

Next, we evaluate the second-order structure function of this field, calculated for a separation of a single footprint in the x direction (i.e. perpendicular to the strips), with the differences illustrated in Figure S10 (a,b). At a separation of one footprint the variance of LES differences, i.e. $S_2(\Delta r$=1 grid cell), is 0.004 mm^2, while the retrieved value is 0.110 mm^2. The next step is to smooth the field in the y direction and then recalculate $S_2(\Delta r$=1 grid cell) in the x direction, as shown in Figure S10 (c). Given the very small spatial variability on this scale, the reduction in retrieved variance, from 0.011 mm^2 to 0.058 mm^2 is almost entirely due to the reduction in σ_ϵ^2. We therefore attribute all reduction in $S_{2,ret}$ after perpendicular smoothing to the σ_ϵ^2 term, and this is the principle behind our main manuscript results.

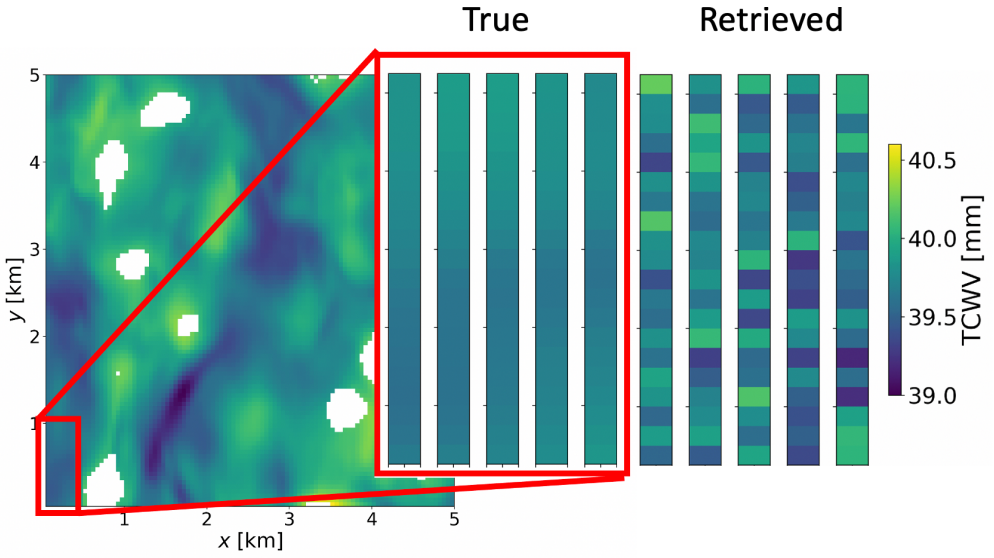

Figure S9. Blown up section of TCWV from a corner of one LES simulation. The red inset shows strips that are one grid-cell wide of the true LES output field next to the retrieved values. Note that the retrieved values are within the same range as that of the LES, but the LES variability takes place over ranges of ~1 km, while the random error is just as large over neighbouring footprints.

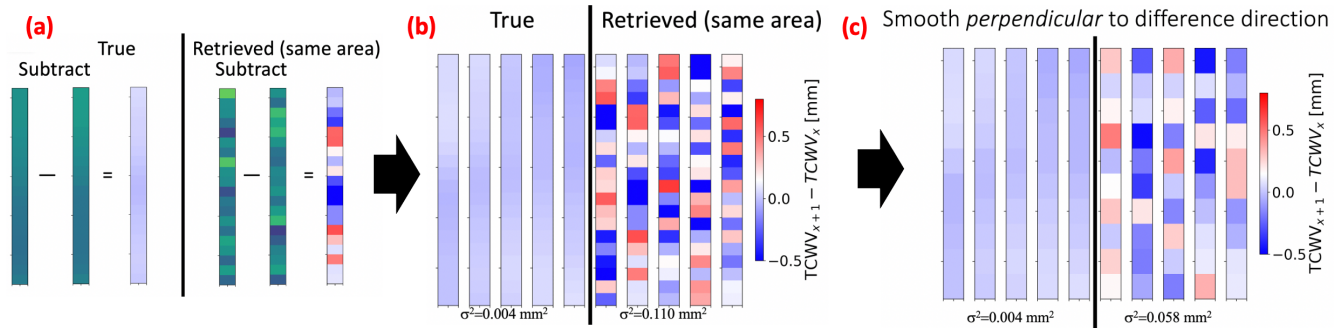

Figure S10. Illustration structure function approach. (a) Subtract each footprint from the footprint to its left to obtain a difference at a separation Δr=1 footprint. (b) calculate the variance of these difference over the full LES (c) smooth the field in the direction perpendicular to which the difference was calculated, and then obtain the new variance.

An alternative is to assume that the field can be captured by some smoothly-varying true TCWV field and random variation. This was the approach adopted for measured radiances in Thompson et al. (2017, see main manuscript for full citation), where a smoothed field $f_{sm}(x,y)$ was generated by using an 11-footprint boxcar filter in one direction, and then the random component $f_{rand}(x,y)$ was estimated from the true field $f(x,y)$ as:

$$f_{rand}(x,y) = f(x,y) - f_{sm}(x,y) \quad \text{(S1)}$$

The variance of $f_{rand}(x,y)$, i.e. σ^2_{rand} was then taken to represent "noise" in the field. However, for our LES where 11 grid cells span ~0.5 km, there is some true TCWV variability such that $\sigma^2_{rand} \neq \sigma^2_\epsilon$. Figure S11 shows how using the Thompson et al. (2017) smoothing approach would result in estimates of σ_ε that are too large in most cases.

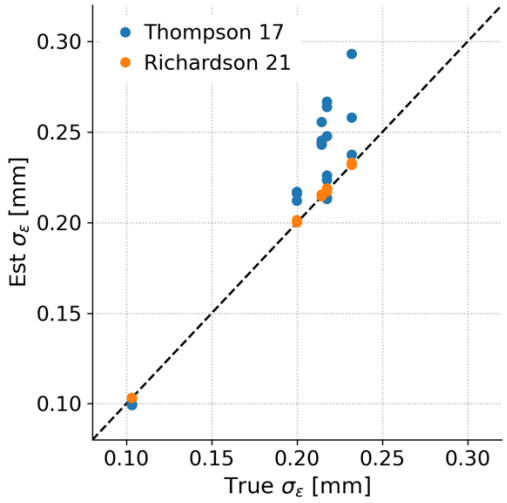

Figure S11. Estimated σ_ε using residuals from a one-dimensional 11-grid moving boxcar filter (Eq. S1, Thompson 17) or this structure function approach (Richardson 21) as a function of the known true σ_ε value from the emulator.

9 Atmospheric sensitivity tests

Results from two tests of how atmospheric conditions affect retrieval sensitivity are in Figure S12. The panel (a) test needs just one snapshot since it uses one set of observations with identical error, meaning that scatter is very small and N=101 is sufficient for calculation of statistics. A DRY snapshot is used since this allows application of the U.S. Standard Atmosphere 1976 LUT, whose maximum possible TCWV is higher than in DRY but lower than in the other cases.

In panel (a), using the warmer tropical atmosphere to develop the LUT means lower retrieved TCWV. This follows qualitative expectations from a simplified model: a warmer atmosphere means more line broadening such lower TCWV is needed to generate a given amount of absorption.

Of relevance for local spatial statistics, the regression slope shows 5 % higher sensitivity when using the tropical LUT rather than the U.S. Standard Atmosphere 1976 LUT. DOAS retrievals exploit how absorption is a logarithmic function of TCWV, such that sensitivity dI/dTCWV is nonlinear. The exact response of the retrieval will also depend on TCWV, channels used and the atmosphere, and test (a) demonstrates that this can affect retrieved statistics.

In panel (b) all BOMEX snapshots are used, and this was selected as BOMEX showed the largest $dTCWV_{ret}/dTCWV$. The larger sample size from all snapshots was needed since in this case the forward model radiances are changed, and the varying retrieval error between simulations of the same footprint results in greater scatter. This shows that when the forward model simply scales the median $q(z)$ profile, that the sensitivity is 9 % lower than when the real profile variation is simulated. This change will likely change further with aerosol or temperature profile changes, but it appears that implementing a LUT approach where variability is constrained to lower altitudes might result in more realistic atmospheric retrievals.

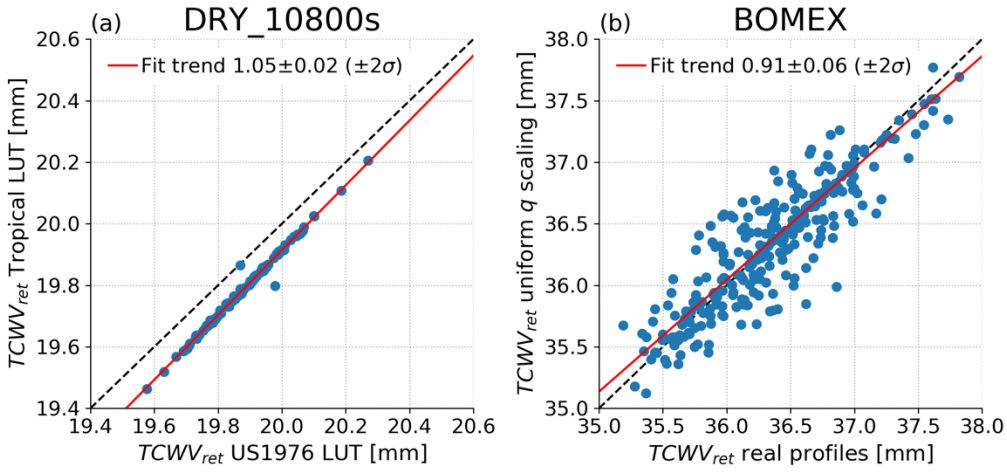

Figure S12. Comparison of pairs of TCWV retrievals, (a) in the DRY_18000s snapshot, results when using the MODTRAN6.0 default tropical atmosphere in the LUT as a function of the results when using the U.S. Standard Atmosphere 1976, (b) for all BOMEX snapshots where each footprint uses the median $q(z)$ profile that is uniformly scaled to match original TCWV, as a function of the default approach using the true LES profiles for each snapshot. Dashed black 1:1 lines are appended, and best fit slopes with ±2σ errors are labelled in the legend.

10 Shifting retrieved field to account for non-vertical solar path

The simulated sunlight follows a downward path at the SZA and a direct upward path. Clearly the downward path is longer due to its horizontal component, and therefore the overall path contains proportionally more downward path than upward path. The vertical profiles $q(z)$ in Figure 1 show that each LES snapshot contains a characteristic layer, typically near the PBL top, at which the majority of TCWV variability occurs. It is therefore fair to ask whether the spatial pattern of $TCWV_{ret}$ will correspond better to the spatial pattern of integrated q at the horizontal location corresponding to where the sunlight passes downward through that layer, as opposed to the TCWV evaluated at the nominal surface footprint.

To assess this, we translated the $TCWV_{ret}$ field towards the incoming sunlight (along the positive y direction) and recalculated the r^2 for translations from 0—2.5 km. Figure S13 shows the results for the ARM_18000s case at native resolution and after smoothing to $\Delta x = 100$ m. There is indeed a peak in correlation coefficient corresponding to the location at which the $TCWV_{ret}$ map lines up with the location at which the downward solar path passes through the layer of largest horizontal q variation. However, the performance is still substantially lower than for SZA=0°. Results are similar for other snapshots, albeit the DRY cases show significantly worse performance.

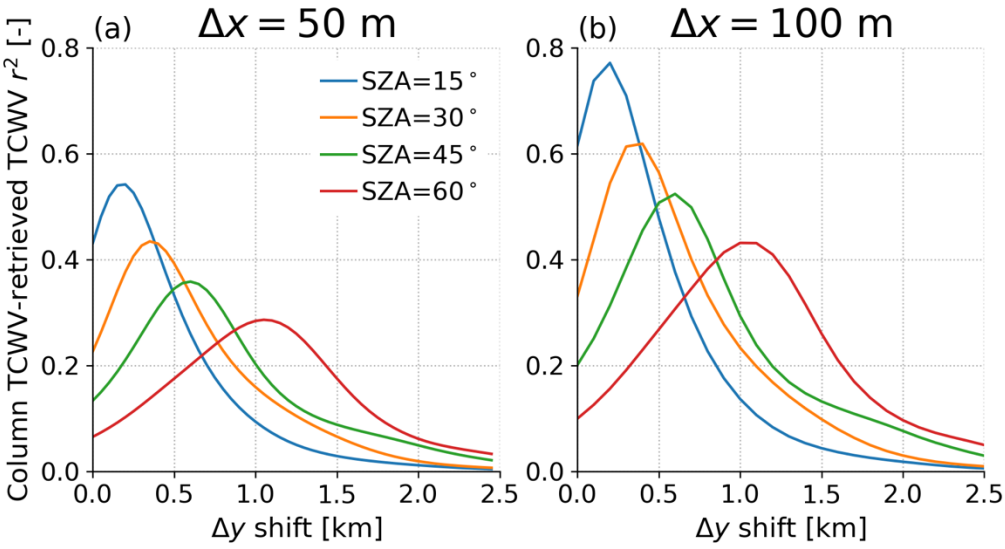

Figure S13. Calculated r^2 between TCWV and TCWVret fields at ARM_18000s as a function of horizontal spatial offset. The $TCWV_{ret}$ field is shifted one footprint at a time in the positive the y direction and r2 is recalculated. Lines show different SZA as labelled in the legend of (a), which contains native resolution output while (b) shows the results when TCWV and $TCWV_{ret}$ are first smoothed to 100 m resolution.